Letter

Generalized many-body exciton *g* factors: Magnetic hybridization and nonmonotonic Rydberg series in monolayer WSe_2

Paulo E. Faria Junior [1,2,3,*,†] Daniel Hernangómez-Pérez [4,*,‡] Tomer Amit [5,*]
Jaroslav Fabian [3] and Sivan Refaely-Abramson [5]

[1]*Department of Physics, University of Central Florida, Orlando, Florida 32816, USA*
[2]*Department of Electrical and Computer Engineering, University of Central Florida, Orlando, Florida 32816, USA*
[3]*Institute of Theoretical Physics, University of Regensburg, 93040 Regensburg, Germany*
[4]*CIC nanoGUNE BRTA, Tolosa Hiribidea 76, 20018 San Sebastián, Spain*
[5]*Department of Molecular Chemistry and Materials Science, Weizmann Institute of Science, Rehovot 7610001, Israel*

(Received 2 June 2025; accepted 5 November 2025; published 3 December 2025)

The magneto-optical response of excitons in monolayer transition metal dichalcogenides is governed by a complex interplay of Bloch-state quantum geometry—reflected in the electronic magnetic moment—coupled with interband mixing and many-body interactions. Here, we develop a robust and general first-principles framework for many-body exciton *g* factors (magnetic moments) by incorporating off-diagonal terms for the spin and orbital angular momenta of single-particle bands and many-body states for magnetic fields pointing in arbitrary spatial directions. We implement our framework using many-body perturbation theory via the GW-Bethe-Salpeter equation and supplement our analysis with robust symmetry-based models. Focusing on the archetypal monolayer WSe_2, we accurately reproduce the known results of the low-energy excitons including the Zeeman splitting and the dark/gray exciton brightening. Furthermore, our theory naturally reveals the magnetic-field hybridization of higher-energy excitons (*s*, *p*, and *d* like) and shows that the magnetic moments of nodal excitons (*p* and *d* like) do not acquire additional contributions of $\pm m_j \mu_B$ ($m_j = 1, 2$), characteristic of the hydrogenic picture. Our general approach also allows us to resolve the long-standing puzzle of the experimentally measured nonmonotonic Rydberg series ($1s - 4s$) of exciton *g* factors. Our framework offers a comprehensive approach to investigate, rationalize, and predict the nontrivial interplay between magnetic fields, angular momenta, and many-body exciton physics in van der Waals systems, offering different opportunities to probe signatures of quantum geometry within many-body states.

DOI: 10.1103/c5y7-w9tk

Introduction. Semiconducting transition metal dichalcogenides (TMDCs) are a family of two-dimensional layered van der Waals materials [1–5] that display unique electronic and optical properties, making them promising candidates for ultrathin optoelectronic, photovoltaic, and valleytronic applications [6–14]. Particularly, optical properties in TMDC systems are dominated by strongly bound excitons—quasiparticles resulting from the electron-hole Coulomb interaction [15–19]. For monolayers, the combination of broken inversion symmetry and strong spin-orbit interaction imprints selective coupling to circularly polarized light at the inequivalent K and $-K$ points in the Brillouin zone [20,21]. As a consequence, direct excitons display valley-dependent optical properties [22,23]. Moreover, excitons carry intrinsic magnetic moments and effectively couple to external magnetic fields, revealing important effects such as many-body Zeeman shifts and magneto-optical selection rule modifications [24–47]. The magnetic moments involved in the exciton magneto-optics are intimately connected to the single-particle quantum geometric tensor [48,49], thus indirectly reflecting the quantum geometry of the underlying electronic Bloch states.

A fundamental framework for understanding magneto-optical exciton phenomena is provided by symmetry-based low-energy model Hamiltonians [50,51]. Such models explain why optically inactive (dark) excitons brighten under in-plane fields in TMDC monolayers due to spin-flip and valley-mixing terms [33,52,53] but do not offer quantitative insights into the coupling terms. Conversely, *ab initio* methods based on the many-body GW-Bethe-Salpeter equation (BSE) [54–57] explicitly include Coulomb interactions and the detailed electronic structure, providing parameter-free information absent in purely symmetry-based models. In particular, the GW-BSE approach captures not only the spatial structure of the single-particle (Bloch) states but also of the excitonic states, achieved by explicitly considering the electron-hole basis and evaluating their many-body interactions. Within this formalism, the microscopic information about the crystal geometry, atomic nature, and orbital details of the wave functions can be incorporated perturbatively to calculate magnetic moments (*g* factors) [38,46,58–60] that reflect underlying quantum geometric effects. However, existing numerical evaluations of exciton *g* factors remain incomplete by neglecting two critical

*These authors contributed equally to this work.
†Contact author: paulo@ucf.edu
‡Contact author: d.hernangomez@nanogune.eu

aspects: (1) insights from group-theory analysis and (2) off-diagonal matrix elements (valley, orbital, and spin mixing) in the electronic and excitonic basis. These limitations severely hinder our ability to understand the fundamental aspects, such as spin-valley mixing, decoherence, and relaxation in realistic systems using reliable *first-principles* techniques.

In this Letter, we present a robust and general first-principles formalism to describe many-body exciton g factors by incorporating off-diagonal elements of spin and orbital angular momenta, both in the single-particle and the exciton basis. These off-diagonal matrix elements are essential for capturing the correct spectral structure in degenerate many-body subspaces and therefore, exciton hybridization under arbitrarily oriented external magnetic fields. We validate our approach by studying the exciton fine structure of monolayer WSe_2, a prototypical TMDC. We reproduce the known results for the low-energy exciton Zeeman splitting and reveal that the brightening of dark/gray excitons in several magnetic field orientations [33,52,53] is a direct consequence of the off-diagonal angular momentum terms. Importantly, we establish that these off-diagonal elements drive the brightening and hybridization of higher-energy excitons (s-p mixing) and that nodal excitons (p and d like) do not acquire additional contributions to the magnetic moments of the type $\pm m_j \mu_B$. Moreover, our approach provides a natural resolution to the long-standing puzzle of the nonmonotonic behavior in the excitonic Rydberg series g factors ($1s-4s$) [36–39]. Our formalism opens different opportunities to investigate and predict the role of many-body effects and quantum geometry signatures on the nontrivial spin-valley physics of excitons in complex van der Waals systems.

General theory of exciton g factors. The Hamiltonian describing two-particle excitations in the presence of an external magnetic field reads $\hat{H} = \hat{H}^{\mathrm{BSE}} + \hat{\mathbf{g}} \cdot \boldsymbol{\mathcal{B}}$ [further details in Sec. II of the Supplemental Material (SM) [61]]. The term $\hat{H}^{\mathrm{BSE}}$ represents the BSE Hamiltonian, $\hat{\mathbf{g}} = (\hat{g}^x, \hat{g}^y, \hat{g}^z)$ corresponds to the g factor, $\mathcal{B}_\epsilon := \mu_B B_\epsilon$, $B_{\epsilon=x,y,z}$ is the external magnetic field, and μ_B the Bohr magneton. In the exciton basis, the BSE Hamiltonian is diagonal, $\langle S|\hat{H}^{\mathrm{BSE}}|S'\rangle = \Omega_S \delta_{S,S'}$, with Ω_S being the exciton energies. The magnetic coupling within degenerate and between different exciton subspaces is driven by the external magnetic field and characterized by the Hamiltonian matrix elements $\langle S|\hat{H}|S'\rangle = \sum_\epsilon g^\epsilon_{SS'} \mathcal{B}_\epsilon$, which are excitonic-dressed "generalized" g-factor matrix elements,

$$g^\epsilon_{SS'} = \sum_{vc\mathbf{k}} \left(\mathcal{A}^S_{vc\mathbf{k}}\right)^* \left[\sum_{c'} \mathcal{A}^{S'}_{vc'\mathbf{k}} g^\epsilon_{cc'\mathbf{k}} - \sum_{v'} \mathcal{A}^{S'}_{v'c\mathbf{k}} g^\epsilon_{vv'\mathbf{k}}\right]. \quad (1)$$

Here, $g^\epsilon_{\alpha\alpha'\mathbf{k}} = \langle \alpha\mathbf{k}|\hat{L}^\epsilon + \hat{\Sigma}^\epsilon|\alpha'\mathbf{k}\rangle$ are the electronic g-factor matrix elements [62] accounting for the direct magnetic coupling, $\hat{L}^\epsilon$ ($\hat{\Sigma}^\epsilon$) the components of the orbital (spin) angular momentum operator in the Bloch basis, $|\alpha\mathbf{k}\rangle$, and $\mathcal{A}^S_{vc\mathbf{k}}$ the exciton amplitude obtained from the solution of the BSE. Equation (1) extends on previous derivations [58,59] by considering off-diagonal terms in the exciton g factor, not only in the excitonic but also in the single-particle electron/hole manifold (band g factors). For the latter, we need to consider off-diagonal matrix elements of single-particle operators in the Bloch basis. For instance, the orbital angular momentum

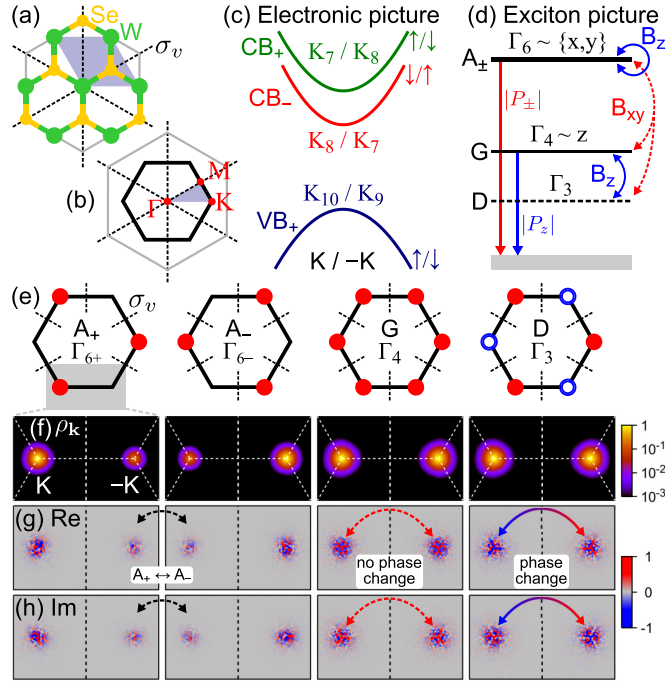

FIG. 1. (a) Top view of the monolayer WSe_2. The colored parallelogram indicates the primitive unit cell. (b) First Brillouin zone. The colored triangle indicates the irreducible wedge. The dashed lines in (a) and (b) indicate the mirror planes σ_v. (c) Low-energy bands at $K/-K$ valleys, including the irreps and spin orientation. (d) Low-energy exciton states at the Γ point, identified by their labeling and irreps (see main text). Vertical arrows indicate the allowed optical transitions. Curved arrows indicate couplings via the magnetic field (solid for $\mathbf{B} \parallel z$ and dashed for $\mathbf{B} \parallel x, y$). (e) Schematic representation of the exciton wave functions. Solid (open) circles indicate positive (negative) amplitudes. For irrep Γ_6, the subindex $+(-)$ refers to the exciton wave function mainly localized in the $+(-)K$ valley. (f) Absolute, (g) real, and (h) imaginary values of the calculated GW-BSE exciton wave functions. The arrows in (g) and (h) emphasize the effect of σ_v, i.e., $\Gamma_{6+}(A_+) \leftrightarrow \Gamma_{6-}(A_-)$, no phase change for Γ_4 (G), and phase change for Γ_3 (D). We adopt the group theory nomenclature of Ref. [64].

in $\hat{\mathbf{z}}$ reads

$$L^z_{\alpha\alpha'\mathbf{k}} = \frac{1}{2im_0}\left[\sum_{\beta\neq\alpha}{}' \frac{p^x_{\alpha\beta\mathbf{k}} p^y_{\beta\alpha'\mathbf{k}} - p^y_{\alpha\beta\mathbf{k}} p^x_{\beta\alpha'\mathbf{k}}}{\epsilon_{\alpha\mathbf{k}} - \epsilon_{\beta\mathbf{k}}} - \sum_{\beta\neq\alpha'}{}' \frac{p^y_{\alpha\beta\mathbf{k}} p^x_{\beta\alpha'\mathbf{k}} - p^x_{\alpha\beta\mathbf{k}} p^y_{\beta\alpha'\mathbf{k}}}{\epsilon_{\alpha'\mathbf{k}} - \epsilon_{\beta\mathbf{k}}}\right], \quad (2)$$

with $p^\epsilon_{\alpha\beta\mathbf{k}} = \langle \alpha\mathbf{k}|\hat{p}^\epsilon|\beta\mathbf{k}\rangle$ [63], i being the imaginary unit, and m_0 the bare electron mass. The prime in the first (second) summation indicates that the α' (α) state must be excluded if α and α' are in the same degenerate subset.

Low-energy excitons. We demonstrate our theoretical approach for the archetypal monolayer WSe_2, extensively studied via magneto-optics [28,33,36–40,52,53,65,66]. The top view of the TMDC crystals (D_{3h} symmetry group) and the first Brillouin zone are depicted in Figs. 1(a) and 1(b), respectively. We focus on the subspace of low-energy

excitons arising from the top valence band, VB_+, and the lowest conduction bands, $CB_\pm$, around the K valleys. Figure 1(c) shows these relevant energy bands, their irreducible representations (irreps), and the direction of the spin expectation value in the out-of-plane direction. The irreps of the direct ($1s$-like) excitons can be obtained by the direct product of K-point irreps and the compatibility relations between K and Γ points [61]. We employ the typical nomenclature for these excitons [33,52,53]: bright ($A \sim \Gamma_6$), gray ($G \sim \Gamma_4$), and dark ($D \sim \Gamma_3$). From the symmetry perspective, A excitons are two-fold degenerate while the D exciton has zero oscillator strength. The resulting low-energy subspace, optical selection rules, and coupling to an external **B** field are summarized in Fig. 1(d), with the schematic representation of the exciton wave functions given in Fig. 1(e).

Our GW-BSE calculations provide the exciton energies and oscillator strengths (Table II in the SM [61]), supplying a clear identification of the low-energy excitons. Notably, the symmetry analysis also allows us to identify the numerical precision of the GW-BSE calculations. The energy values (oscillator strengths) fully satisfy the symmetry constraints up to 0.1 meV ($10^{-3}e^2a_0^2$). The energy splitting between G and A excitons is ~52.4 meV while the D-G splitting is ~2.4 meV, in excellent agreement with experiments in hexagonal boron nitride (hBN)-encapsulated samples [33,52,53,67]. To verify the symmetry features shown in Fig. 1(e) at the GW-BSE level, we display in Figs. 1(f)–1(h) the density ($\rho^S_{\mathbf{k}} = \sum_{vc} |\mathcal{A}^S_{vc\mathbf{k}}|^2$), real ($\mathrm{Re}\{\mathcal{A}^S_{\mathbf{k}}\} = \sum_{vc} \mathrm{Re}\{\mathcal{A}^S_{vc\mathbf{k}}\}$), and imaginary ($\mathrm{Im}\{\mathcal{A}^S_{\mathbf{k}}\} = \sum_{vc} \mathrm{Im}\{\mathcal{A}^S_{vc\mathbf{k}}\}$) values of the computed *ab initio* exciton wave functions. Because of the numerical degeneracy in the A exciton subspace, the wave functions are not fully localized in $\pm K$ but are still connected by the mirror plane σ_v. State mixing is present in first-principles calculations whenever the irreps are (nearly) numerically degenerate [68,69] and must be treated accordingly, specifically by incorporating off-diagonal matrix elements. The symmetry features of G and D excitons is visible in the real and imaginary parts, evidenced by the dashed (G) and solid (D) arrows.

Knowing the excitons' symmetry allows us to incorporate the effect of external magnetic fields (pseudovectors). The resulting symmetry-allowed couplings in the low-energy excitons are shown in Fig. 1(d), revealing that out-of-plane fields ($\mathbf{B} \parallel z \sim \Gamma_2$) yield Zeeman splitting physics for the A exciton subset and mixing of D/G excitons, while in-plane fields ($\mathbf{B} \parallel x, y \sim \Gamma_5$) introduce exciton mixing between A and D/G states. We emphasize here the relevance of our general formalism: mixing effects can only be captured by off-diagonal matrix elements and are relevant for degenerate subsets such as the A exciton. The details of the symmetry analysis and connection to the microscopic contributions of electron g-factors in the exciton basis are given in the SM [61]. We incorporate the magnetic field within GW-BSE by numerically evaluating Eq. (1), including the **k**-space extension of the exciton wave functions coupled via the full matrices Σ and L.

Figure 2 summarizes the main findings for the low-energy exciton subspace. Figures 2(a) and 2(b) show the Zeeman splitting of A and D/G excitons for different magnetic field orientations (θ), revealing that the exciton couplings between degenerate and nondegenerate subsets are properly implemented within our general *ab initio* formalism, in agreement

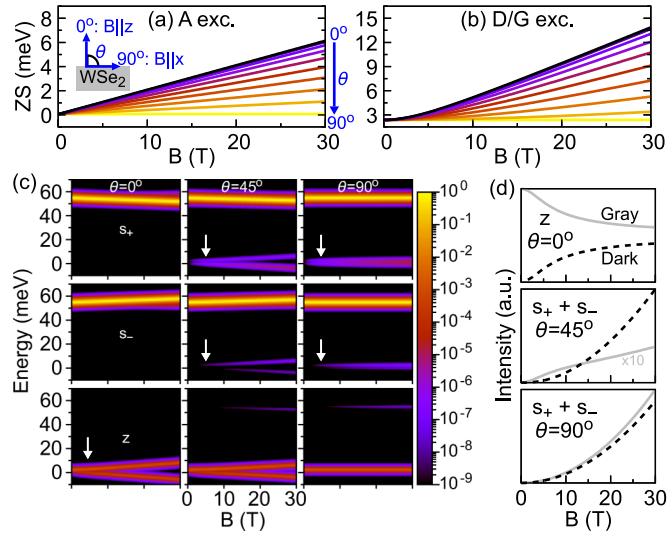

FIG. 2. GW-BSE calculations for the Zeeman splitting of the low-energy excitons under applied magnetic field at different angles, θ, for (a) A and (b) D/G excitons. (c) Calculated absorption via GW-BSE under applied magnetic field oriented at different angles ($\theta = 0°, 45°, 90°$) for s_+ (top row), s_- (middle row), and z (bottom row) polarizations. The spectra are normalized to the maximum value of the s_+ emission. For each transition, a broadening was applied using a sech function with 1 meV full width at half maximum. The vertical arrows highlight important brightening signatures. (d) Intensity dependence for D/G excitons as a function of the magnetic field extracted from (c).

with symmetry-based models [61]. In Fig. 2(c) we present the calculated absorption spectra in logarithmic scale for $\theta = 0°, 45°, 90°$. Our calculations reproduce all the relevant magnetic-hybridization mechanisms observed in photoluminescence experiments (vertical arrows): (1) brightening of D excitons for out-of-plane fields [33]; (2) brightening of D excitons for tilted fields [52]; and (3) brightening of both D and G excitons for in-plane fields [53]. Figure 2(d) summarizes the explicit magnetic-field dependence of these brightening features. We note that photoluminescence experiments incorporate the exciton occupation, given by a Boltzmann distribution function [70] with rapid exponential decay[71]. We emphasize that the exciton brightening under magnetic fields is a direct consequence of the off-diagonal elements of the spin and orbital angular momenta, incorporated in the generalized exciton g-factor formalism of Eq. (1). The comparison between the full GW-BSE calculations and symmetry-based models is given in the SM [61].

Magnetic-hybridization of high-energy excitons. While low-energy excitons are easily described by effective models, high-energy excitons (often called *excited* excitons) pose a greater challenge due to the increasingly denser excitonic manifold of available states with enhanced intervalley exchange and spin-orbital mixing. To emphasize the significance of the exciton hybridization at higher energies, we present in Figs. 3(a) and 3(b) the absolute values of the out-of-plane and in-plane g factors for the lowest 20 excitons (see the SM [61] for a larger exciton subset). Notably, both g-factor components display significant presence of off-diagonal elements

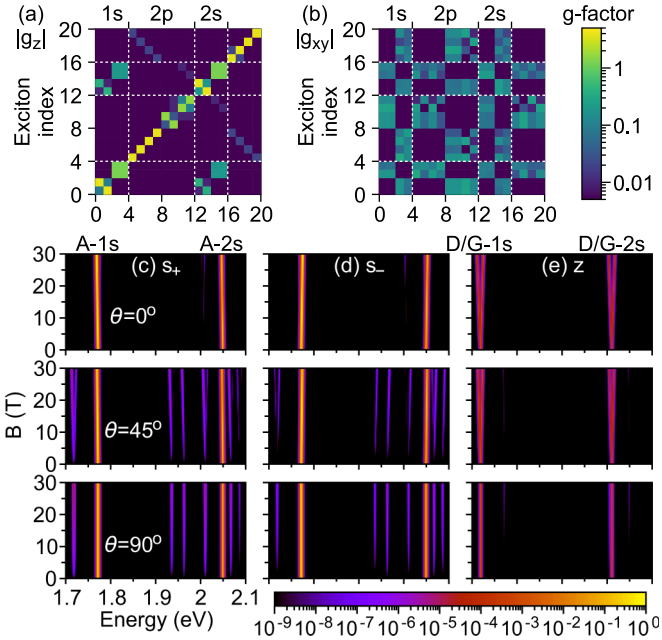

FIG. 3. Absolute value of the (a) out-of-plane g-factor matrix, $|g_z|$, and (b) in-plane g-factor matrix, $|g_{xy}| = \sqrt{g_x^2 + g_y^2}$, via Eq. (1), as a function of the exciton index, demonstrating the significance of the off-diagonal terms. Calculated absorption as a function of the magnetic field oriented at different angles ($\theta = 0°, 45°, 90°$) for (c) s_+, (d) s_-, and (e) z polarizations. The values are normalized to the maximum value of the s_+ emission. We apply the same broadening as in Fig. 2. Several exciton peaks emerge around 1.95 eV, visible for $\theta = 45°, 90°$. We consider the nonzero oscillator strengths only for s-like exciton states.

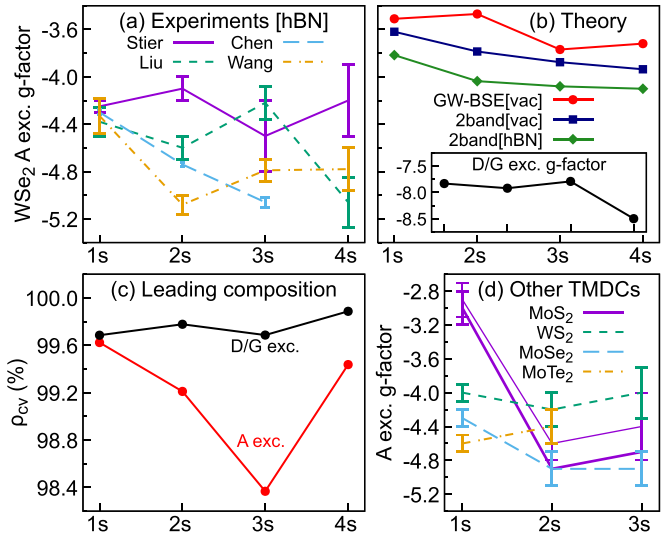

FIG. 4. (a) Experimental g factors of the Rydberg series ($1s - 4s$) of the A exciton by Stier *et al.* [36], Liu *et al.* [37], Chen *et al.* [38], and Wang *et al.* [39]. (b) Calculated g factors via the GW-BSE approach (circles), using an effective two-band model (squares), and via the two-band model considering hBN encapsulation (diamonds). Notably, the observed nonmonotonic trends can only be accurately reproduced using our *ab initio* GW-BSE generalized g-factor theory. Inset: g factors of D/G Rydberg excitons, also exhibiting nonmonotonic features. (c) Leading composition of the exciton wave function, $\rho_{vc}^S = \sum_{\mathbf{k}} |A_{vc\mathbf{k}}^S|^2$, for A ($v = 1, c = 2$) and D/G ($v = 1, c = 1$) excitons. (d) Experimental g factors of the Rydberg series of the A exciton for other TMDCs by Goryca *et al.* [74], revealing consistent nonmonotonic features.

responsible for hybridizing states that belong to different exciton subspaces, completely absent in previous studies [58,59]. Moreover, g-factors of p-like (and d-like [61]) excitons have similar magnitude as their s-like counterparts, revealing that nodal excitons *do not* acquire additional contributions to the magnetic moments of the type $\pm m_j \mu_B$, as one would expect from a hydrogen-atom picture.

In Figs. 3(c)–3(e) we display the calculated absorption for $s_\pm$ and z polarization for the exciton subset shown in Figs. 3(a) and 3(b). For $s_\pm$ polarizations, external magnetic fields lead to the brightening of several optically inactive excitonic states. In particular, we reveal a clear signature of the mixing of s-p excitons, recently observed by external in-plane electric fields in monolayer WSe_2 [72]. For z-polarized light, we recover the brightening of the excited D/G states [see Fig. 2(c)]. Similar to the recently proposed s-p mixing of excitons in van der Waals heterostructures [73], this brightening cannot be captured by purely (Wannier or symmetry-based) effective models, underscoring the importance of including the full complexity of the excitonic spectrum using the generalized GW-BSE treatment.

Rydberg series of g factors. To showcase the robust capabilities of our approach, we address the long-standing puzzle and conflicting experimental reports of the Rydberg series of the A exciton g factors for the so-called $1s - 4s$ states. Figure 4(a) compiles the available experimental g factors in hBN-encapsulated monolayer WSe_2 from Refs. [36–39], revealing an overall decreasing trend together with clear nonmonotonic signatures, varying slightly due to sample-dependent factors [75–77].

In Fig. 4(b), we present our calculated g factors via the full *ab initio* GW-BSE approach, revealing that nonmonotonic features naturally emerge from our formalism. Notably, the g factors for D/G Rydberg excitons also exhibit nonmonotonic dependencies [see the inset of Fig. 4(b)]. We also evaluate the g factors using an effective (parabolic) two-band model incorporating the dielectric screening of vacuum and hBN encapsulation (see Sec. I of the SM [61]). The effective model systematically yields a monotonic behavior and fails to reproduce the oscillations obtained in the GW-BSE g-factor calculations via Eq. (1). These nonmonotonic features cannot be explained by simplified models but naturally emerge from our generalized GW-BSE formalism, which incorporates orbital and spin mixing induced by external magnetic fields.

To highlight the nontrivial effects present in our general formalism, Fig. 4(c) displays the leading composition of the exciton wave function. These values are quite high, around 99.7% for D/G excitons and in between 98.4% and 99.6% for the A excitons. Although these results would strongly suggest that effective two-band models would be capable of describing the relevant exciton g-factor physics, particularly for D/G excitons, Figure 4(b) shows otherwise. Moreover, the nonmonotonic features of Rydberg excitons are not limited to WSe_2,

but are also present in other TMDCs, namely MoS_2, $MoSe_2$, $MoTe_2$, and WS_2. In Fig. 4(d) we present the experimental g factors collected from Ref. [74], revealing the general presence of the nonmonotonic signatures in the Rydberg series of the A exciton. Our results firmly indicate that the interplay between the excitonic fine structure and magnetic response is highly nontrivial and strongly dependent on the exciton state, emphasizing the need for first-principles-based approaches when interpreting high-resolution magneto-optical measurements.

Conclusions and outlook. In this Letter, we developed a robust and general framework based on *ab initio* many-body GW-BSE formalism that incorporates the interplay of the spin and orbital angular momenta via the exciton g factors. This approach takes into account the hybridization of single-particle bands and many-body states through off-diagonal matrix elements of spin and orbital angular momenta. We validate our approach for the archetypal TMDC monolayer WSe_2, capturing and rationalizing the observed results of the exciton Zeeman splitting as well as brightening of the optically dark/gray excitons by in-plane/tilted magnetic fields. We also explore the brightening of high-energy excitons, a challenging task for pure symmetry-based models, emphasizing that many-body off-diagonal components of the g factor are crucial to capture the magnetic mixing of exciton states. These results imply that interpreting high-energy features in magneto-optics requires caution, as nominally distinct excitonic subspaces can strongly hybridize. Equally important, we reveal that excited p- and d-like excitons do not acquire additional contributions of the type $\pm m_j \mu_B$ ($m_j = 1, 2$) to their magnetic moments. Furthermore, the robustness of our approach allows us to recover the nonmonotonic behavior of the Rydberg series of exciton g factors, a long-standing puzzle observed experimentally not only in WSe_2 [36–39], but also visible in other monolayer TMDCs [74].

Beyond enabling the study of nontrivial excitonic spin-valley-orbital dynamics [78] and unconventional topological and chiral excitons [79,80], our methodology opens different avenues for uncovering elusive quantum phenomena driven by the interplay of crystal symmetry, quantum geometry, and many-body effects in complex two-dimensional materials and van der Waals heterostructures. Furthermore, our framework holds significant promise for the emerging field of orbitronics [81], offering a pathway to deeper insights into the impact of many-body interactions on orbital degrees of freedom in low-dimensional systems, and providing valuable guidance for magneto-optical spectroscopy exploiting composite many-body exciton complexes [42,82–85].

Acknowledgments. The authors acknowledge the financial support of the Deutsche Forschungsgemeinschaft (DFG, German Research Foundation) SFB 1277 (Project No. 314695032). P.E.F.J. acknowledges the computational resources of the Advanced Research Computing Center of the University of Central Florida. D.H.-P. acknowledges the funding from the Diputación Foral de Gipuzkoa through Grants No. 2023-FELL-000002-01 and No. 2024-FELL-000009-01, from the Spanish MICIU/AEI/10.13039/501100011033 and FEDER, UE through Project No. PID2023-147324NA-I00, and the computational resources of the Max Planck Computing and Data Facility (MPCDF) cluster. T.A. acknowledges support from the Azrieli Graduate Fellows Program. S.R.-A. acknowledges a European Research Council (ERC) Starting Grant No. 101041159.

Data availability. The data that support the findings of this article are not publicly available. The data are available from the authors upon reasonable request.

[1] Q. H. Wang, K. Kalantar-Zadeh, A. Kis, J. N. Coleman, and M. S. Strano, Electronics and optoelectronics of two-dimensional transition metal dichalcogenides, Nat. Nanotechnol. **7**, 699 (2012).

[2] A. K. Geim and I. V. Grigorieva, Van der Waals heterostructures, Nature (London) **499**, 419 (2013).

[3] K. S. Novoselov, A. Mishchenko, A. Carvalho, and A. H. C. Neto, 2D materials and van der Waals heterostructures, Science **353**, aac9439 (2016).

[4] Y. Liu, N. O. Weiss, X. Duan, H.-C. Cheng, Y. Huang, and X. Duan, Van der Waals heterostructures and devices, Nat. Rev. Mater. **1**, 16042 (2016).

[5] S. Manzeli, D. Ovchinnikov, D. Pasquier, O. V. Yazyev, and A. Kis, 2D transition metal dichalcogenides, Nat. Rev. Mater. **2**, 17033 (2017).

[6] B. Radisavljevic, A. Radenovic, J. Brivio, V. Giacometti, and A. Kis, Single-layer MoS_2 transistors, Nat. Nanotechnol. **6**, 147 (2011).

[7] O. López-Sánchez, D. Lembke, M. Kayci, A. Radenovic, and A. Kis, Ultrasensitive photodetectors based on monolayer MoS_2, Nat. Nanotechnol. **8**, 497 (2013).

[8] D. Jariwala, V. K. Sangwan, L. J. Lauhon, T. J. Marks, and M. C. Hersam, Emerging device applications for semiconducting two-dimensional transition metal dichalcogenides, ACS Nano **8**, 1102 (2014).

[9] A. Pospischil, M. M. Furchi, and T. Mueller, Solar-energy conversion and light emission in an atomic monolayer p–n diode, Nat. Nanotechnol. **9**, 257 (2014).

[10] F. Withers, O. Del Pozo-Zamudio, A. Mishchenko, A. P. Rooney, A. Gholinia, K. Watanabe, T. Taniguchi, S. J. Haigh, A. K. Geim, A. I. Tartakovskii, and K. S. Novoselov, Light-emitting diodes by band-structure engineering in van der Waals heterostructures, Nat. Mater. **14**, 301 (2015).

[11] J. R. Schaibley, H. Yu, G. Clark, P. Rivera, J. S. Ross, K. L. Seyler, W. Yao, and X. Xu, Valleytronics in 2D materials, Nat. Rev. Mater. **1**, 16055 (2016).

[12] Z. Ye, D. Sun, and T. F. Heinz, Optical manipulation of valley pseudospin, Nat. Phys. **13**, 26 (2017).

[13] K. F. Mak and J. Shan, Photonics and optoelectronics of 2D semiconductor transition metal dichalcogenides, Nat. Photon. **10**, 216 (2016).

[14] K. F. Mak, D. Xiao, and J. Shan, Light–valley interactions in 2D semiconductors, Nat. Photon. **12**, 451 (2018).

[15] K. F. Mak, C. Lee, J. Hone, J. Shan, and T. F. Heinz, Atomically thin MoS_2: A new direct-gap semiconductor, Phys. Rev. Lett. **105**, 136805 (2010).

[16] A. Splendiani, L. Sun, Y. Zhang, T. Li, J. Kim, C.-Y. Chim, G. Galli, and F. Wang, Emerging photoluminescence in monolayer MoS_2, Nano Lett. **10**, 1271 (2010).

[17] D. Y. Qiu, F. H. da Jornada, and S. G. Louie, Optical spectrum of MoS_2: Many-body effects and diversity of exciton states, Phys. Rev. Lett. **111**, 216805 (2013).

[18] A. Chernikov, T. C. Berkelbach, H. M. Hill, A. Rigosi, Y. Li, B. Aslan, D. R. Reichman, M. S. Hybertsen, and T. F. Heinz, Exciton binding energy and nonhydrogenic Rydberg series in monolayer WS_2, Phys. Rev. Lett. **113**, 076802 (2014).

[19] G. Wang, A. Chernikov, M. M. Glazov, T. F. Heinz, X. Marie, T. Amand, and B. Urbaszek, *Colloquium*: Excitons in atomically thin transition metal dichalcogenides, Rev. Mod. Phys. **90**, 021001 (2018).

[20] T. Cao, G. Wang, W. Han, H. Ye, C. Zhu, J. Shi, Q. Niu, P. Tan, E. Wang, B. Liu, and J. Feng, Valley-selective circular dichroism of monolayer molybdenum disulphide, Nat. Commun. **3**, 887 (2012).

[21] D. Xiao, G.-B. Liu, W. Feng, X. Xu, and W. Yao, Coupled spin and valley physics in monolayers of MoS_2 and other group-VI dichalcogenides, Phys. Rev. Lett. **108**, 196802 (2012).

[22] G. Sallen, L. Bouet, X. Marie, G. Wang, C. R. Zhu, W. P. Han, Y. Lu, P. H. Tan, T. Amand, B. L. Liu, and B. Urbaszek, Robust optical emission polarization in MoS_2 monolayers through selective valley excitation, Phys. Rev. B **86**, 081301(R) (2012).

[23] K. F. Mak, K. He, J. Shan, and T. F. Heinz, Control of valley polarization in monolayer MoS_2 by optical helicity, Nat. Nanotechnol. **7**, 494 (2012).

[24] Y. Li, J. Ludwig, T. Low, A. Chernikov, X. Cui, G. Arefe, Y. D. Kim, A. M. van der Zande, A. Rigosi, H. M. Hill, S. H. Kim, J. Hone, Z. Li, D. Smirnov, and T. F. Heinz, Valley splitting and polarization by the Zeeman effect in monolayer $MoSe_2$, Phys. Rev. Lett. **113**, 266804 (2014).

[25] D. MacNeill, C. Heikes, K. F. Mak, Z. Anderson, A. Kormányos, V. Zólyomi, J. Park, and D. C. Ralph, Breaking of valley degeneracy by magnetic field in monolayer $MoSe_2$, Phys. Rev. Lett. **114**, 037401 (2015).

[26] G. Wang, L. Bouet, M. Glazov, T. Amand, E. Ivchenko, E. Palleau, X. Marie, and B. Urbaszek, Magneto-optics in transition metal diselenide monolayers, 2D Mater. **2**, 034002 (2015).

[27] A. Srivastava, M. Sidler, A. V. Allain, D. S. Lembke, A. Kis, and A. Imamoğlu, Valley Zeeman effect in elementary optical excitations of monolayer WSe_2, Nat. Phys. **11**, 141 (2015).

[28] G. Aivazian, Z. Gong, A. M. Jones, R.-L. Chu, J. Yan, D. G. Mandrus, C. Zhang, D. Cobden, W. Yao, and X. Xu, Magnetic control of valley pseudospin in monolayer WSe_2, Nat. Phys. **11**, 148 (2015).

[29] A. Mitioglu, P. Plochocka, Á. Granados del Aguila, P. Christianen, G. Deligeorgis, S. Anghel, L. Kulyuk, and D. Maude, Optical investigation of monolayer and bulk tungsten diselenide (WSe_2) in high magnetic fields, Nano Lett. **15**, 4387 (2015).

[30] A. V. Stier, K. M. McCreary, B. T. Jonker, J. Kono, and S. A. Crooker, Exciton diamagnetic shifts and valley Zeeman effects in monolayer WS_2 and MoS_2 to 65 Tesla, Nat. Commun. **7**, 10643 (2016).

[31] A. V. Stier, N. P. Wilson, G. Clark, X. Xu, and S. A. Crooker, Probing the influence of dielectric environment on excitons in monolayer WSe_2: Insight from high magnetic fields, Nano Lett. **16**, 7054 (2016).

[32] R. Schmidt, A. Arora, G. Plechinger, P. Nagler, A. Granados del Águila, M. V. Ballottin, P. C. M. Christianen, S. Michaelis de Vasconcellos, C. Schüller, T. Korn, and R. Bratschitsch, Magnetic-field-induced rotation of polarized light emission from monolayer WS_2, Phys. Rev. Lett. **117**, 077402 (2016).

[33] C. Robert, T. Amand, F. Cadiz, D. Lagarde, E. Courtade, M. Manca, T. Taniguchi, K. Watanabe, B. Urbaszek, and X. Marie, Fine structure and lifetime of dark excitons in transition metal dichalcogenide monolayers, Phys. Rev. B **96**, 155423 (2017).

[34] X.-X. Zhang, T. Cao, Z. Lu, Y.-C. Lin, F. Zhang, Y. Wang, Z. Li, J. C. Hone, J. A. Robinson, D. Smirnov, S. G. Louie, and T. F. Heinz, Magnetic brightening and control of dark excitons in monolayer WSe_2, Nat. Nanotechnol. **12**, 883 (2017).

[35] A. Arora, M. Koperski, A. Slobodeniuk, K. Nogajewski, R. Schmidt, R. Schneider, M. R. Molas, S. M. de Vasconcellos, R. Bratschitsch, and M. Potemski, Zeeman spectroscopy of excitons and hybridization of electronic states in few-layer WSe_2, $MoSe_2$ and $MoTe_2$, 2D Mater. **6**, 015010 (2018).

[36] A. V. Stier, N. P. Wilson, K. A. Velizhanin, J. Kono, X. Xu, and S. A. Crooker, Magnetooptics of exciton Rydberg states in a monolayer semiconductor, Phys. Rev. Lett. **120**, 057405 (2018).

[37] E. Liu, J. van Baren, T. Taniguchi, K. Watanabe, Y.-C. Chang, and C. H. Lui, Magnetophotoluminescence of exciton Rydberg states in monolayer WSe_2, Phys. Rev. B **99**, 205420 (2019).

[38] S.-Y. Chen, Z. Lu, T. Goldstein, J. Tong, A. Chaves, J. Kunstmann, L. S. R. Cavalcante, T. Woźniak, G. Seifert, D. R. Reichman, T. Taniguchi, K. Watanabe, D. Smirnov, and J. Yan, Luminescent emission of excited Rydberg excitons from monolayer WSe_2, Nano Lett. **19**, 2464 (2019).

[39] T. Wang, Z. Li, Y. Li, Z. Lu, S. Miao, Z. Lian, Y. Meng, M. Blei, T. Taniguchi, K. Watanabe, S. Tongay, D. Smirnov, C. Zhang, and S.-F. Shi, Giant valley-polarized Rydberg excitons in monolayer WSe_2 revealed by magneto-photocurrent spectroscopy, Nano Lett. **20**, 7635 (2020).

[40] C. Robert, H. Dery, L. Ren, D. Van Tuan, E. Courtade, M. Yang, B. Urbaszek, D. Lagarde, K. Watanabe, T. Taniguchi, T. Amand, and X. Marie, Measurement of conduction and valence bands *g*-factors in a transition metal dichalcogenide monolayer, Phys. Rev. Lett. **126**, 067403 (2021).

[41] M. Zinkiewicz, T. Woźniak, T. Kazimierczuk, P. Kapuscinski, K. Oreszczuk, M. Grzeszczyk, M. Bartoš, K. Nogajewski, K. Watanabe, T. Taniguchi, C. Faugeras, P. Kossacki, M. Potemski, A. Babiński, and M. R. Molas, Excitonic complexes in n-doped WS_2 monolayer, Nano Lett. **21**, 2519 (2021).

[42] A. Arora, Magneto-optics of layered two-dimensional semiconductors and heterostructures: Progress and prospects, J. Appl. Phys. **129**, 120902 (2021).

[43] P. E. Faria Junior, K. Zollner, T. Woźniak, M. Kurpas, M. Gmitra, and J. Fabian, First-principles insights into the spin-valley physics of strained transition metal dichalcogenides monolayers, New J. Phys. **24**, 083004 (2022).

[44] F. S. Covre, P. E. Faria Junior, V. O. Gordo, C. S. de Brito, Y. V. Zhumagulov, M. D. Teodoro, O. D. D. Couto, L. Misoguti, S. Pratavieira, M. B. Andrade, P. C. M. Christianen, J. Fabian, F. Withers, and Y. G. Gobato, Revealing the impact of strain in the optical properties of bubbles in monolayer $MoSe_2$, Nanoscale **14**, 5758 (2022).

[45] E. Blundo, P. E. Faria Junior, A. Surrente, G. Pettinari, M. A. Prosnikov, K. Olkowska-Pucko, K. Zollner, T. Woźniak, A. Chaves, T. Kazimierczuk, M. Felici, A. Babiński, M. R. Molas, P. C. M. Christianen, J. Fabian, and A. Polimeni, Strain-induced exciton hybridization in WS_2 monolayers unveiled by Zeeman-splitting measurements, Phys. Rev. Lett. **129**, 067402 (2022).

[46] P. E. Faria Junior, T. Naimer, K. M. McCreary, B. T. Jonker, J. J. Finley, S. A. Crooker, J. Fabian, and A. V. Stier, Proximity-enhanced valley Zeeman splitting at the WS_2/graphene interface, 2D Mater. **10**, 034002 (2023).

[47] K. Olkowska-Pucko, T. Woźniak, E. Blundo, N. Zawadzka, Łucja Kipczak, P. E. Faria Junior, J. Szpakowski, G. Krasucki, S. Cianci, D. Vaclavkova, D. Jana, P. Kapuściński, M. Grzeszczyk, D. Cecchetti, G. Pettinari, I. Antoniazzi, Z. Sofer, I. Plutnarová, K. Watanabe, T. Taniguchi *et al.*, Extremely high excitonic g-factors in 2D crystals by alloy-induced admixing of band states, arXiv:2503.23071.

[48] J. P. Provost and G. Vallee, Riemannian structure on manifolds of quantum states, Commun. Math. Phys. **76**, 289 (1980).

[49] Ó. P. Ocaña and I. Souza, Multipole theory of optical spatial dispersion in crystals, SciPost Phys. **14**, 118 (2023).

[50] K. Cho, Unified theory of symmetry-breaking effects on excitons in cubic and wurtzite structures, Phys. Rev. B **14**, 4463 (1976).

[51] H. Venghaus, S. Suga, and K. Cho, Magnetoluminescence and magnetoreflectance of the A exciton of CdS and CdSe, Phys. Rev. B **16**, 4419 (1977).

[52] M. R. Molas, C. Faugeras, A. O. Slobodeniuk, K. Nogajewski, M. Bartos, D. M. Basko, and M. Potemski, Brightening of dark excitons in monolayers of semiconducting transition metal dichalcogenides, 2D Mater. **4**, 021003 (2017).

[53] M. R. Molas, A. O. Slobodeniuk, T. Kazimierczuk, K. Nogajewski, M. Bartos, P. Kapuściński, K. Oreszczuk, K. Watanabe, T. Taniguchi, C. Faugeras, P. Kossacki, D. M. Basko, and M. Potemski, Probing and manipulating valley coherence of dark excitons in monolayer WSe_2, Phys. Rev. Lett. **123**, 096803 (2019).

[54] M. S. Hybertsen and S. G. Louie, Electron correlation in semiconductors and insulators: Band gaps and quasiparticle energies, Phys. Rev. B **34**, 5390 (1986).

[55] M. Rohlfing and S. G. Louie, Electron-hole excitations in semiconductors and insulators, Phys. Rev. Lett. **81**, 2312 (1998).

[56] S. Albrecht, L. Reining, R. Del Sole, and G. Onida, *Ab initio* calculation of excitonic effects in the optical spectra of semiconductors, Phys. Rev. Lett. **80**, 4510 (1998).

[57] X. Blase, I. Duchemin, D. Jacquemin, and P.-F. Loos, The Bethe–Salpeter equation formalism: From physics to chemistry, J. Phys. Chem. Lett. **11**, 7371 (2020).

[58] T. Deilmann, P. Krüger, and M. Rohlfing, *Ab initio* studies of exciton g factors: Monolayer transition metal dichalcogenides in magnetic fields, Phys. Rev. Lett. **124**, 226402 (2020).

[59] T. Amit, D. Hernangómez-Pérez, G. Cohen, D. Y. Qiu, and S. Refaely-Abramson, Tunable magneto-optical properties in MoS_2 via defect-induced exciton transitions, Phys. Rev. B **106**, L161407 (2022).

[60] L. Kipczak, A. O. Slobodeniuk, T. Woźniak, M. Bhatnagar, N. Zawadzka, K. O. Pucko, M. J. Grzeszczyk, K. Watanabe, T. Taniguchi, A. Babinski, and M. Molas, Analogy and dissimilarity of excitons in monolayer and bilayer of $MoSe_2$, 2D Mater. **10**, 025014 (2023).

[61] See Supplemental Material at http://link.aps.org/supplemental/10.1103/c5y7-w9tk for the computational details, the representation of spin and orbital operators in the excitonic basis, the symmetry analysis, additional computational data, and additional figures, which includes Refs. [33,43,46,52–55,58,59,60,64,68,69,86–115].

[62] In this form, the g-factor is simply the total angular momentum, $\mathbf{J} = \mathbf{L} + \mathbf{S}$ with spin-orbit effects incorporated via the basis functions.

[63] Nonlocal effects in the band g factors [116,117] are not considered. We focus on the combined effect of the excitonic properties within nearly degenerate subspaces.

[64] G. F. Koster, J. O. Dimmock, R. G. Wheeler, and H. Statz, *Properties of the Thirty-Two Point Groups* (MIT press, Cambridge, MA, 1963), Vol. 24.

[65] M. Koperski, K. Nogajewski, A. Arora, V. Cherkez, P. Mallet, J.-Y. Veuillen, J. Marcus, P. Kossacki, and M. Potemski, Single photon emitters in exfoliated WSe_2 structures, Nat. Nanotechnol. **10**, 503 (2015).

[66] K.-Q. Lin, C. S. Ong, S. Bange, P. E. Faria Junior, B. Peng, J. D. Ziegler, J. Zipfel, C. Bäuml, N. Paradiso, K. Watanabe, T. Taniguchi, C. Strunk, B. Monserrat, J. Fabian, A. Chernikov, D. Y. Qiu, S. G. Louie, and J. M. Lupton, Narrow-band high-lying excitons with negative-mass electrons in monolayer WSe_2, Nat. Commun. **12**, 5500 (2021).

[67] G. Wang, C. Robert, M. M. Glazov, F. Cadiz, E. Courtade, T. Amand, D. Lagarde, T. Taniguchi, K. Watanabe, B. Urbaszek, and X. Marie, In-plane propagation of light in transition metal dichalcogenide monolayers: Optical selection rules, Phys. Rev. Lett. **119**, 047401 (2017).

[68] J. V. V. Cassiano, A. de Lelis Araújo, P. E. Faria Junior, and G. J. Ferreira, DFT2kp: Effective kp models from *ab-initio* data, SciPost Physics Codebases **25**, (2024).

[69] S. Zhang, H. Sheng, Z.-D. Song, C. Liang, Y. Jiang, S. Sun, Q. Wu, H. Weng, Z. Fang, X. Dai *et al.*, VASP2KP: $k \cdot p$ models and Landé g-factors from *ab initio* calculations, Chin. Phys. Lett. **40**, 127101 (2023).

[70] Y. V. Zhumagulov, A. Vagov, D. R. Gulevich, P. E. Faria Junior, and V. Perebeinos, Trion induced photoluminescence of a doped MoS_2 monolayer, J. Chem. Phys. **153**, 044132 (2020).

[71] In photoluminescence spectra, the A, G, and D excitons display similar intensities [33,52,53,66,118] due to their distinct occupation, also influenced by the aperture of the objective lens used to collect the emitted light [66].

[72] B. Zhu, K. Xiao, S. Yang, K. Watanabe, T. Taniguchi, and X. Cui, In-plane electric-field-induced orbital hybridization of excitonic states in monolayer WSe_2, Phys. Rev. Lett. **131**, 036901 (2023).

[73] J. D. Cao, K. S. Denisov, and I. Zutic, Tunable resonant s-p mixing of excitons in van der Waals heterostructures, Phys. Rev. B **112**, L161405 (2025).

[74] M. Goryca, J. Li, A. V. Stier, T. Taniguchi, K. Watanabe, E. Courtade, S. Shree, C. Robert, B. Urbaszek, X. Marie, and S. A. Crooker, Revealing exciton masses and dielectric properties of monolayer semiconductors with high magnetic fields, Nat. Commun. **10**, 4172 (2019).

[75] L. Mennel, M. M. Furchi, S. Wachter, M. Paur, D. K. Polyushkin, and T. Mueller, Optical imaging of strain in two-dimensional crystals, Nat. Commun. **9**, 516 (2018).

[76] A. Raja, L. Waldecker, J. Zipfel, Y. Cho, S. Brem, J. D. Ziegler, M. Kulig, T. Taniguchi, K. Watanabe, E. Malic, T. F. Heinz, T. C. Berkelbach, and A. Chernikov, Dielectric disorder in two-dimensional materials, Nat. Nanotechnol. **14**, 832 (2019).

[77] P. V. Kolesnichenko, Q. Zhang, T. Yun, C. Zheng, M. S. Fuhrer, and J. A. Davis, Disentangling the effects of doping, strain and disorder in monolayer WS_2 by optical spectroscopy, 2D Mater. **7**, 025008 (2020).

[78] S. Raiber, P. E. Faria Junior, D. Falter, S. Feldl, P. Marzena, K. Watanabe, T. Taniguchi, J. Fabian, and C. Schüller, Ultrafast pseudospin quantum beats in multilayer WSe_2 and $MoSe_2$, Nat. Commun. **13**, 4997 (2022).

[79] B. Hou, D. Wang, B. A. Barker, and D. Y. Qiu, Exchange-driven intermixing of bulk and topological surface states by chiral excitons in Bi_2Se_3, Phys. Rev. Lett. **130**, 216402 (2023).

[80] H.-Y. Xie, P. Ghaemi, M. Mitrano, and B. Uchoa, Theory of topological exciton insulators and condensates in flat Chern bands, Proc. Natl. Acad. Sci. USA **121**, e2401644121 (2024).

[81] T. P. Cysne, L. M. Canonico, M. Costa, R. B. Muniz, and T. G. Rappoport, Orbitronics in two-dimensional materials, npj Spintron. **3**, 39 (2025).

[82] D. Van Tuan and H. Dery, Composite excitonic states in doped semiconductors, Phys. Rev. B **106**, L081301 (2022).

[83] D. Van Tuan, S.-F. Shi, X. Xu, S. A. Crooker, and H. Dery, Six-body and eight-body exciton states in monolayer WSe_2, Phys. Rev. Lett. **129**, 076801 (2022).

[84] J. Choi, J. Li, D. Van Tuan, H. Dery, and S. A. Crooker, Emergence of composite many-body exciton states in WS_2 and $MoSe_2$ monolayers, Phys. Rev. B **109**, L041304 (2024).

[85] A. Dijkstraa, A. B. Mhenni, D. V. Tuan, E. Çetiner, M. Schur-Wilkens, J. Kim, L. Steiner, K. Watanabe, T. Taniguchi, M. Barbone, N. P. Wilson, H. Dery, and J. J. Finley, Ten-valley excitonic complexes in charge-tunable monolayer WSe_2, Nat. Commun. **16**, 9743 (2025).

[86] W. Schutte, J. De Boer, and F. Jellinek, Crystal structures of tungsten disulfide and diselenide, J. Solid State Chem. **70**, 207 (1987).

[87] M. Camarasa-Gómez, A. Ramasubramaniam, J. B. Neaton, and L. Kronik, Transferable screened range-separated hybrid functionals for electronic and optical properties of van der Waals materials, Phys. Rev. Mater. **7**, 104001 (2023).

[88] P. Giannozzi, S. Baroni, N. Bonini, M. Calandra, R. Car, C. Cavazzoni, D. Ceresoli, G. L. Chiarotti, M. Cococcioni, I. Dabo, A. Dal Corso, S. de Gironcoli, S. Fabris, G. Fratesi, R. Gebauer, U. Gerstmann, C. Gougoussis, A. Kokalj, M. Lazzeri, L. Martin-Samos *et al.*, QUANTUM ESPRESSO: A modular and open-source software project for quantum simulations of materials, J. Phys.: Condens. Matter **21**, 395502 (2009).

[89] P. Giannozzi, O. Andreussi, T. Brumme, O. Bunau, M. Buongiorno Nardelli, M. Calandra, R. Car, C. Cavazzoni, D. Ceresoli, M. Cococcioni, N. Colonna, I. Carnimeo, A. Dal Corso, S. de Gironcoli, P. Delugas, R. A. DiStasio, A. Ferretti, A. Floris, G. Fratesi, G. Fugallo *et al.*, Advanced capabilities for materials modelling with QUANTUM ESPRESSO, J. Phys.: Condens. Matter **29**, 465901 (2017).

[90] P. Giannozzi, O. Baseggio, P. Bonfà, D. Brunato, R. Car, I. Carnimeo, C. Cavazzoni, S. de Gironcoli, P. Delugas, F. Ferrari Ruffino, A. Ferretti, N. Marzari, I. Timrov, A. Urru, and S. Baroni, QUANTUM ESPRESSO toward the exascale, J. Chem. Phys. **152**, 154105 (2020).

[91] J. P. Perdew, K. Burke, and M. Ernzerhof, Generalized gradient approximation made simple, Phys. Rev. Lett. **77**, 3865 (1996).

[92] M. J. van Setten, M. Giantomassi, E. Bousquet, M. J. Verstraete, D. R. Hamann, X. Gonze, and G.-M. Rignanese, The PseudoDojo: Training and grading a 85 element optimized norm-conserving pseudopotential table, Comput. Phys. Commun. **226**, 39 (2018).

[93] P. Blaha, K. Schwarz, F. Tran, R. Laskowski, G. K. Madsen, and L. D. Marks, WIEN2k: An APW+lo program for calculating the properties of solids, J. Chem. Phys. **152**, 074101 (2020).

[94] K. Lejaeghere, G. Bihlmayer, T. Björkman, P. Blaha, S. Blügel, V. Blum, D. Caliste, I. E. Castelli, S. J. Clark, A. D. Corso, S. de Gironcoli, T. Deutsch, J. K. Dewhurst, I. D. Marco, C. Draxl, M. Dułak, O. Eriksson, J. A. Flores-Livas, K. F. Garrity, L. Genovese *et al.*, Reproducibility in density functional theory calculations of solids, Science **351**, aad3000 (2016).

[95] D. J. Singh and L. Nordstrom, *Planewaves, Pseudopotentials, and the LAPW method* (Springer Science & Business Media, New York, 2006).

[96] J. Deslippe, G. Samsonidze, D. A. Strubbe, M. Jain, M. L. Cohen, and S. G. Louie, BerkeleyGW: A massively parallel computer package for the calculation of the quasiparticle and optical properties of materials and nanostructures, Comput. Phys. Commun. **183**, 1269 (2012).

[97] M. Rohlfing and S. G. Louie, Electron-hole excitations and optical spectra from first principles, Phys. Rev. B **62**, 4927 (2000).

[98] M. Wu, Spin-Orbit coupling, broken time-reversal symmetry, and polarizability self-consistency in GW and GW-BSE theory with applications to two-dimensional materials, Ph.D. thesis, University of California, Berkeley, 2020.

[99] B. A. Barker, J. Deslippe, J. Lischner, M. Jain, O. V. Yazyev, D. A. Strubbe, and S. G. Louie, Spinor *GW*/Bethe-Salpeter calculations in BerkeleyGW: Implementation, symmetries, benchmarking, and performance, Phys. Rev. B **106**, 115127 (2022).

[100] F. H. da Jornada, D. Y. Qiu, and S. G. Louie, Nonuniform sampling schemes of the Brillouin zone for many-electron perturbation-theory calculations in reduced dimensionality, Phys. Rev. B **95**, 035109 (2017).

[101] S. Ismail-Beigi, Truncation of periodic image interactions for confined systems, Phys. Rev. B **73**, 233103 (2006).

[102] T. Woźniak, P. E. Faria Junior, G. Seifert, A. Chaves, and J. Kunstmann, Exciton *g*-factors of van der Waals heterostructures from first-principles calculations, Phys. Rev. B **101**, 235408 (2020).

[103] N. S. Rytova, Screened potential of a point charge in a thin film, Moscow Univ. Phys. Bull. **3**, 30 (1967).

[104] L. V. Keldysh, Coulomb interaction in thin semiconductor and semimetal films, JETP Lett. **29**, 658 (1979).

[105] A. Laturia, M. L. Van de Put, and W. G. Vandenberghe, Dielectric properties of hexagonal boron nitride and transition

metal dichalcogenides: From monolayer to bulk, npj 2D Mater. Appl. **2**, 6 (2018).

[106] Y. G. Gobato, C. S. de Brito, A. Chaves, M. A. Prosnikov, T. Woźniak, S. Guo, I. D. Barcelos, M. V. Milošević, F. Withers, and P. C. M. Christianen, Distinctive g-factor of moiré-confined excitons in van der Waals heterostructures, Nano Lett. **22**, 8641 (2022).

[107] J. Ruan, Z. Li, C. S. Ong, and S. G. Louie, Optically controlled single-valley exciton doublet states with tunable internal spin structures and spin magnetization generation, Proc. Natl. Acad. Sci. USA **120**, e2307611120 (2023).

[108] J. J. Esteve-Paredes, M. A. García-Blázquez, A. J. Uría-Álvarez, M. Camarasa-Gómez, and J. J. Palacios, Excitons in nonlinear optical responses: Shift current in MoS_2 and GeS monolayers, npj Comput. Mater. **11**, 13 (2025).

[109] Y. Yafet, *G* factors and spin-lattice relaxation of conduction electrons, *Solid State Physics* (Elsevier, Amsterdam, 1963), Vol. 14.

[110] S. Bhowal and G. Vignale, Orbital Hall effect as an alternative to valley Hall effect in gapped graphene, Phys. Rev. B **103**, 195309 (2021).

[111] A. Urru, O. P. O. Ivo Souza, S. S. Tsirkin, and D. Vanderbilt, Optical spatial dispersion via Wannier interpolation, arXiv:2504.09742.

[112] M. M. Glazov, T. Amand, X. Marie, D. Lagarde, L. Bouet, and B. Urbaszek, Exciton fine structure and spin decoherence in monolayers of transition metal dichalcogenides, Phys. Rev. B **89**, 201302(R) (2014).

[113] H. Dery and Y. Song, Polarization analysis of excitons in monolayer and bilayer transition-metal dichalcogenides, Phys. Rev. B **92**, 125431 (2015).

[114] M. Kurpas, M. Gmitra, and J. Fabian, Spin-orbit coupling and spin relaxation in phosphorene: Intrinsic versus extrinsic effects, Phys. Rev. B **94**, 155423 (2016).

[115] M. Kurpas, P. E. Faria Junior, M. Gmitra, and J. Fabian, Spin-orbit coupling in elemental two-dimensional materials, Phys. Rev. B **100**, 125422 (2019).

[116] F. Xuan and S. Y. Quek, Valley Zeeman effect and Landau levels in two-dimensional transition metal dichalcogenides, Phys. Rev. Res. **2**, 033256 (2020).

[117] F. Xuan and S. Y. Quek, Valley-filling instability and critical magnetic field for interaction-enhanced Zeeman response in doped WSe_2 monolayers, npj Comput. Mater. **7**, 198 (2021).

[118] F. Dirnberger, J. D. Ziegler, P. E. Faria Junior, R. Bushati, T. Taniguchi, K. Watanabe, J. Fabian, D. Bougeard, A. Chernikov, and V. M. Menon, Quasi-1D exciton channels in strain-engineered 2D materials, Sci. Adv. **7**, eabj3066 (2021).